A WALL INTERFERENCE ASSESSMENT/CORRECTION SYSTEM

SEMI-ANNUAL REPORT #1

Dr. C.F. Lo, Principal Investigator
University of Tennessee Space Institute

Covering the period June 1991 through December 1991

Under NASA Ames Research Center NAG 2-733

Ames Research Center
Moffett Field, CA 94035-1000

INSTITUTION:

CSTAR - Center for Space
Transportation and Applied Research
UTSI Research Park
Tullahoma, TN 37388-8897

Phone 615-455-9294 or 5884

Title: A Wall Interference Assessment/Correction System

Semi-Annual Report
June - December, 1991

Principal Investigator:
Dr. C. F. Lo, UTSI

Other Investigators:
Dr. J. C. Erickson, CSTAR
Mr. N. Ulbrich, GRA/UTSI

Technical Officer:
Dr. Frank W. Steinle, NASA/Ames Research Center

Technical Objectives

The Hackett method--a Wall Pressure Signature method has been selected to be adapted for the 12-ft Wind Tunnel WIAC system in the present phase. This method uses limited measurements of the static pressure at the wall, in conjunction with the solid wall boundary condition, to determine the strength and distribution of singularities representing the test article. The singularities are used in turn for estimating wall interference at the model location. Hackett's method will have to be formulated for application to the unique geometry of the 12-ft Tunnel. The development and implementation of a working prototype will be completed, delivered and documented with a software manual in this phase.

The WIAC code will be validated by conducting numerically simulated experiments rather actual wind tunnel experiments. It is an effective, but efficient way to validate the implemented code. The simulations will be used to generate both free-air and confined wind-tunnel flow fields for each of the test articles over a range of test configurations. Specifically, the pressure signature at the test section wall will be computed for the confined case to provide the simulated "measured" data. These data will serve as the input for the WIAC method--Hackett's method in this phase. The performance of the WIAC method then may be evaluated by comparing the corrected parameters with those for the free-air simulation. Each set of wind tunnel/test article numerical simulations provides data to validate the WIAC method.

Status of Progress

1. System Validation Design

A numerical wind tunnel test simulation is planned to be utilized to validate the WIAC methods developed in the project, specifically to the wall pressure signature method--Hackett's method in the current phase. A low-order potential-flow panel method has been selected to simulate the wind tunnel and test article geometries for its flexibility.

A copy of the low-order panel code, called PMARC (Panel Method Ames Research Center), was obtained from Dr. Frank Steinle, technical monitor. The code of PMARC (Ref. 1) is a well-documented code with open architecture which has several advanced features including internal flow modeling for wind tunnel application. The code has another feature allowing the adjustment of the size of panel for suiting the computer hardware and the size of the problem. PMARC can be run on computers ranging from a MacIntosh II workstation to a Cray Y-MP.

Currently, the copy of PMARC (version 12) has been compiled on a IBM R6000 and checked out on two sample cases -- wing and wing/body which have been provided by NASA/ARC. The PMAPP, a post processor for PMARC, will be received from NASA/ARC shortly.

2. Hackett's Method Implementation

The implementation of a Wall Pressure Signature method which is based upon the wall interference method developed by Hackett (Ref. 2) has been initiated. In the present reported period, the blockage correction is developed and implemented. The lifting correction will be carried out in the next period. A working computer code has been implemented and verified by an analytic solution.

The analytic flow field solution of a rectangular wind tunnel with a finite airfoil wing and its wake was derived as a bench mark solution to verify the solution calculated by Hackett's Method. The blockage correction of the Wall Pressure Signature method (Hackett's Method) for this wing/wake case is obtained and verified by the analytical solution.

The detailed development and results are given in Attachment I.

Future Plan

1. Panel Code Application

The application of panel code PMARC will be initiated for Ames 12-ft Wind Tunnel. The wall pressure in using Hackett's method will be computed for the cases of wing and wing/body configuration. The post processor (PMAPP) for PMARC will be installed on the UTSI's computer to support PMARC's application. The software system validation will be started for Hackett's method developed in Task 2 with the configuration of 12-ft Tunnel.

2. Lifting Correction of Hackett's Method

The development and implementation of the lifting Correction of Hackett's Method will be initiated. The verification will be based on an independent solution such as a corresponding solution of lifting case derived in this reported period for the blockage case.

References

1. Ashby, D.L. et al, "Potential Flow Theory and Operation Guide for the Panel Code PMARC," NASA Tech. Memo 102851, January 1991

2. Hackett, J. E. et al, "A Review of the Wall Pressure Signature and other Tunnel Constraint Correction Methods for High Angle-of-Attacks Tests", AGARD Report No. 692, May 1980

Attachment I

NASA Ames Research Center NAG 2-733

BLOCKAGE CORRECTION IN 3-DIMENSIONAL WIND TUNNEL TESTING BASED ON THE WALL SIGNATURE METHOD

BLOCKAGE CORRECTION IN 3-DIMENSIONAL WIND TUNNEL TESTING BASED ON THE WALL SIGNATURE METHOD

N. Ulbrich and C. F. Lo
The University of Tennessee Space Institute
Tullahoma, Tennessee 37388

Summary

A blockage correction technique in 3-dimensional wind tunnel flow fields is developed and verified. Blockage corrections are obtained by Hackett's method with pressure measurements on the wind tunnel wall.

An analytic wind tunnel flow field solution of a rectangular wing with parabolic airfoil section and a trailing edge wake is presented. This analytic solution is used to simulate pressure measurements on selected wall locations and to calculate the exact solution of the blockage problem.

A pressure coefficent correction due to model blockage is obtained by Hackett's method in using simulated wall pressure measurements. Pressure coefficient corrections show good agreement with the exact solution of the blockage correction problem. This verifies the implementation of Hackett's method for the blockage correction.

1. Introduction

The Wall Pressure Signature Technique (Hackett's method)[1,2,3,4,5] is considered to calculate blockage correction due to wall interference in the NASA/ARC 12ft Pressure Wind Tunnel. The first part of this report presents the development and implementation of an analytical correction technique which requires the simulation of wall pressure measurements for Hackett's method. A wind tunnel with rectangular cross section is selected. A rectangular wing with parabolic airfoil section is chosen as a test article and a solution of this flow field is obtained by applying thin wing theory. The influence of the wake is modeled by using a line source and a line sink. The analytic solution of the wind tunnel flow field of a wing and a wake is obtained by combining free-air solutions with the method of images.

Two important sets of data are derived from the analytic solution: wall pressure measurements are simulated which will be used as required by Hackett's method to calculate blockage corrections; the exact solution of the blockage problem is calculated to verify Hackett's method. Basic steps of the development and verification of a blockage correction technique based on wall pressure measurements are shown in Fig. 1.

A detailed description of Hackett's method is presented in the second part of this report. It is shown how an equivalent flow field representation is defined based on wall pressure measurements. This equivalent flow field model is then used in combination with the method of images to calculate a blockage correction. This blockage correction is compared to the exact solution of the blockage problem to verify Hackett's method.

2. Analytic Wind Tunnel Flow Field

2.1 General Remarks

The simulation of a three dimensional wind tunnel flow field requires the mathematical description of a simplified test article and a wake. A rectangular wing with parabolic airfoil section is selected as a test article. In general the analytic solution of a wing in incompressible three-dimensional flow cannot be obtained easily. Integration of complicated algebraic expressions is necessary.

The solution of the thickness problem of a thin wing in incompressible free-air flow is known in the form of a double integral. Basic equations will be presented and the geometry of the selected rectangular tunnel and wing will be specified. The free air solution is obtained by direct integration. A wake in free-air flow can be simulated by using a finite span line source and line sink. An analytic flow field solution will be derived by direct integration as well.

The wind tunnel flow field will be calculated by superimposing the analytic solutions of wing and wake and applying the method of images to the total flow field to satisfy the wall boundary conditions.

Finally formulae of the analytic solution of the blockage problem are obtained.

2.2 Free-Air Flow Field of the Wing

The solution of the perturbation potential of three-dimensional planar wings in incompressible free-air flow is given by *Ashley and Landahl*[6] as follows

$$\varphi_1(x,y,z) \;=\; -\frac{\tau}{2\pi}\cdot\iint\limits_{A}\frac{\partial g(x_1,y_1)}{\partial x_1}\cdot\frac{dx_1\;dy_1}{\sqrt{(x-x_1)^2+(y-y_1)^2+z^2}} \tag{1}$$

where 'A' is the projected wing area, 'τ' is the thickness and $\partial g(x_1,y_1)/\partial x_1$ is the thickness slope.

Figure 2 shows a rectangular wing with parabolic airfoil section, wing span 's' and chord length 'c'. The thickness function $g(x_1,y_1)$ of the parabolic airfoil section has the following form

$$g(x_1,y_1) \;=\; 2\cdot x_1\cdot\left[1-\frac{x_1}{c}\right] \tag{2a}$$

The thickness slope is then given as

$$\frac{\partial g(x_1,y_1)}{\partial x_1} \;=\; \frac{\partial g(x_1)}{\partial x_1} \;=\; 2\cdot\left[1-\frac{2x_1}{c}\right] \tag{2b}$$

Combining Eqs.(1), (2b) and knowing that $0\le x_1\le c$ and $-s/2\le y_1\le s/2$ we get

$$\varphi_1(x,y,z) \;=\; -\frac{\tau}{\pi}\cdot\int_0^c\int_{-s/2}^{s/2}\frac{[1-2x_1/c]}{\sqrt{(x-x_1)^2+(y-y_1)^2+z^2}}\;dx_1\;dy_1 \tag{3}$$

The dimensionless axial perturbation velocity is given as

$$u_1(x,y,z) = \frac{\partial \varphi_1}{\partial x} = \frac{\tau}{\pi} \cdot \int_0^c \int_{-s/2}^{s/2} \frac{[1-2x_1/c]\cdot(x-x_1)}{[(x-x_1)^2+(y-y_1)^2+z^2]^{3/2}}\, dx_1\, dy_1 \qquad (4)$$

or in terms of the corresponding pressure coefficient

$$c_{p_1}(x,y,z) = -2 \cdot u_1(x,y,z) \qquad (5)$$

The integration of Eq.(4) is complicated. Different types of integrals have to be considered depending on the choice of field point.

In general the solution consists of six cases to cover the entire flow field. The classification of these cases and the solution of the incompressible axial perturbation velocity are given in *Appendix A*. Singularities exist at the leading and trailing edge of the wing. Otherwise a well defined solution can be found in the flow field.

A verification of parts of the solution is possible if the limit as the wing span goes to infinity is taken. The axial perturbation velocity on the model surface is obtained based on Eq. (A.3) and limits given in *Appendix B*. We get

$$\lim_{s\to\infty} u(x,y,0) = \frac{4}{\pi} \cdot \tau \cdot \left(1 + \frac{1}{2} \cdot [1-2x/c] \cdot \ln \frac{|x/c|}{|1-x/c|}\right) \qquad (6)$$

Equation (6) agrees with the solution of a two-dimensional parabolic airfoil section given by *Schlichting and Truckenbrodt*[7].

Pressure coefficients in free-air on selected locations are calculated based on Eq. (5) and the analytic solution given in the *Appendix A*. The following wing geometry is chosen: chord length $c = 1.0$, wing span $s = 4.0$, thickness $\tau = 0.1$. Pressure coefficients are calculated on the planes $z = 0.0, 0.2$. Results are presented in Figs. (3a) and (3b).

Singularities on the leading and trailing edge of the wing can be noticed in Fig. (3a). It is obvious that the pressure coefficient distribution is symmetric with respect to the planes $y = 0.0$ and $x = c/2$. This symmetry property can be used to reduce calculation time if pressure coefficients in a plane with constant z-coordinate are determined. The absolute value of the pressure coefficient decreases with inceasing z-coordinate as the perturbations of the free-air flow field decay with increasing distance from the wing plane.

2.3 Free-Air Flow Field of the Trailing Edge Wake

The flow field of the trailing edge wake of a rectangular wing is simulated using a line source located on the trailing edge and a line sink of equal strength at a large distance 'c_s' downstream of the trailing edge. The geometry of the wake model is given in Fig. (4).

The general solution of the velocity potential of a single line source of span 'b_w' and constant source strength 'q' in free-air flow is given by *Katz and Plotkin*[8] as

$$\varphi(x,y,z) \;=\; -\frac{q}{4\pi}\cdot\int_{l_1}^{l_2}\frac{dl}{\sqrt{(x-x_1)^2+(y-y_1)^2+(z-z_1)^2}} \tag{7a}$$

We now consider a line source and a line sink located in the x-y plane as shown in Fig. 4. In this case we get for the potential the following equation

$$\begin{aligned}\varphi_2(x,y,z) \;=\; &-\frac{q}{4\pi}\cdot\int_{-b_w/2}^{b_w/2}\frac{dy_1}{\sqrt{(x-x_s)^2+(y-y_1)^2+z^2}}\\ &+\frac{q}{4\pi}\cdot\int_{-b_w/2}^{b_w/2}\frac{dy_1}{\sqrt{(x-x_s-c_s)^2+(y-y_1)^2+z^2}}\end{aligned} \tag{7b}$$

The axial perturbation velocity $u_2(x,y,z)$ can now be obtained by diffentiating potential φ_2 with respect to x. We get then

$$u_2(x,y,z) \;=\; \frac{\partial\varphi_2}{\partial x} \tag{8a}$$

or

$$\begin{aligned}u_2(x,y,z) \;=\; &-\frac{q}{4\pi}\cdot[x-x_s]\int_{y+b_w/2}^{y-b_w/2}\frac{d\xi}{[(x-x_s)^2+z^2+\xi^2]^{3/2}}\\ &+\frac{q}{4\pi}\cdot[x-x_s-c_s]\int_{y+b_w/2}^{y-b_w/2}\frac{d\xi}{[(x-x_s-c_s)^2+z^2+\xi^2]^{3/2}}\end{aligned} \tag{8b}$$

The complete analytic solution of the free-air solution of a wake is given in *Appendix C*. The source/sink strength 'q' is equal to the wake thickness 'd_w' if 'u_2' is dimensionless.

2.4 Wall Pressure Measurements and Blockage

The solution of the axial perturbation velocity of a rectangular wing and a trailing edge wake in a rectangular wind tunnel of width W and height H (see Fig. 2) can be derived if the method of images is combined with the free-air solution. The tunnel solution is obtained by superimposing free-air solutions as follows:

$$\begin{aligned}u_T(x,y,z) \;=\; &\sum_{m=-\infty}^{\infty}\sum_{n=-\infty}^{\infty}u_1(x,y+mW,z+nH)\\ &+\sum_{m=-\infty}^{\infty}\sum_{n=-\infty}^{\infty}u_2(x,y+mW,z+nH)\end{aligned} \tag{9a}$$

where the velocity 'u_1' is given by Eqs.(A.1) ... (A.5) in *Appendix A* and velocity 'u_2' is given by Eqs.(C.1) and (C.2) in *Appendix C*. It is only necessary to substitute 'y' by '$y + mW$' and 'z' by '$z + nH$' in these equations.
For practical calculations Eq. (9a) is approximated as follows

$$u_T(x,y,z) \approx \sum_{m=-k}^{k} \sum_{n=-k}^{k} u_1(x, y+mW, z+nH) + \sum_{m=-k}^{k} \sum_{n=-k}^{k} u_2(x, y+mW, z+nH) \qquad (9b)$$

where 'k' has to be a large number to guarantee convergence of the solution. The corresponding pressure coefficient in the flow field is given as

$$c_{p_T}(x,y,z) = -2 \cdot u_T(x,y,z) \qquad (9c)$$

A computer cannot represent numbers exactly and errors are introduced due to finite digit arithmetic. The wind tunnel flow field of the wing is considered alone to study this problem. The wing geometry of the free-air study, a tunnel width $W = 6.0$ and a tunnel height $H = 4.0$ are selected. A single point in the flow field is chosen ($x = 0.5$, $y = 0.0$, $z = 0.2$) and the pressure coefficient is plotted as a function of the chosen summation limit 'k' (see Fig. (5)). The single precision solution becomes unstable at $k \approx 8$. The double precision solution converges uniformly.

Figure 6 shows a specific wind tunnel,wake and wing geometry. For this case pressure coefficients are calculated in the plane $z = 1.75$ (upper wind tunnel wall). Results are presented in Fig. 7. It is now possible to simulate input data for the application of Hackett's method if a single row on the tunnel wall is selected (e.g. $y = 0.0$ and $z = 1.75$). Wall pressure coefficients are calculated on 31 different locations on this row. Calculated results are depicted as the solid line in Fig. 8.

The verification of blockage corrections obtained by Hackett's method requires a comparison with the exact solution of the blockage problem. The exact solution of the blockage problem of the given superimposed flow field can be calculated based on the free-air and wind tunnel solutions. This correction on the plane $z = 0$ is defined as follows

$$c_{p_i}(x,y,0) = c_{p_T}(x,y,0) - c_p(x,y,0) \qquad (10a)$$

where c_{p_T} is given by Eq. (9c). The free-air pressure coefficient is calculated based on Eqs. (4) and (8b) as follows

$$c_p = -2 \cdot [\, u_1 + u_2] \qquad (10b)$$

The calcuation of the pressure coefficient correction has to be done in double precision arithmetic to achieve sufficient accuracy.

The blockage correction c_{p_i} is now calculated for a single row on the surface of the model ($y = 0$). These results are depicted as the solid line in Fig. (9). This analytic solution of the blockage problem will be used to verify Hackett's method.

3. Hackett's Method

3.1 General Remarks

Wall pressure signature methods like Hackett's method were successfully applied in the past to calculate blockage corrections in 3-dimensional wind tunnel testing. Hackett's method consists of two major parts: the signature analysis of the wall pressure measurements to model test articles and the calculation of blockage corrections based on the simplified test article representation obtained from the signature analysis.

At first a description of the signature analysis will be presented. The signature analysis is applied to a simulated wall signature which is calculated for a given wing, wake and wind tunnel geometry as shown in Fig. 6. Secondly the simplified model/wake representation is derived. Finally, blockage corrections are calculated based on the simplified model representation and the method of images which are compared to the exact solution of the blockage problem.

3.2 Signature Analysis

These simulated measurements of a selected model/wake/wind tunnel geometry are obtained from the analytic solution described in Section 2.4 . Simulated wall pressure coefficients on a selected wind tunnel wall (i.e. $-2.5 \leq y \leq 2.5$ and $z = 1.75$) are given in Fig. 7. The signature analysis suggested by *Hackett*[2] is applied to simulated wall pressure measurements on a single row (in our case $y = 0.0$ and $z = 1.75$; see Fig. 6).

The wall pressure measurement on the selected row (solid line in Fig. 8) is split into a symmetric and antisymmetric part by iteration. This iteration requires that the peak location of the symmetric signal is identical with the location of the inflection point of the antisymmetric signal.

The symmetric part of the signal is related to a simplified representation of the solid body blockage in the form of a line source/sink pair. The source/sink spacing and location and the source sink strength can be determined from the width at half height of the symmetric signal, the location of the velocity peak and the maximum value of the velocity.

The antisymmetric part is similarly related to a simplified representation of the wake. Characteristic parameters (like line source/sink location and source/sink strength) are derived from the location of the inflection point of the antisymmetric signal and the asymptotic value of the velocity far downstream of the model. More details on the signature analysis are given by *Hackett*[2]. A concise description of the method is also given by *Allmaras*[5].

3.3 Blockage Correction

Blockage corrections are now calculated based on the simplified test article and wake representation which is given in terms of 4 line sources/sinks. The equations of the blockage correction of the simplified test article and wake representation can be derived easily by modifying equations presented in *Appendix C* and using the method of images. The result of this calculation is given by the dashed line in Fig. 9 and compares well to the known

analytic solution of the blockage problem. Pressure coefficient corrections given in Fig. 9 have to be combined with wind tunnel measurements on the same location in the x-y-z coordinate system to obtain the free-air measurements.

4. Remarks

Blockage corrections in a 3-dimensional wind tunnel flow field are calculated applying Hackett's method to simulated wall pressure measurements. These corrections show excellent agreement with the known analytic solution of the blockage problem. The influence of a fuselage on the applicability of Hackett's method still has to be included in these preliminary results. An improvement of the signature analysis is also considered to simplify the calculation of the equivalent test article and wake representation.

References

[1]Hackett, J. E., Wilsden, D. J., "Determination of Low Speed Wake Blockage Corrections via Tunnel Wall Static Pressure Measurements", AGARD CP-174, October 1975.

[2]Hackett, J. E., Wilsden, D. J. and Lilley, D. E., "Estimation of Tunnel Blockage from Wall Pressure Signatures: A Review and Data Correlation", NASA CR-152241, March 1979.

[3]Hackett, J. E., Wilsden, D. J. and Stevens, W. A., "A Review of the Wall Pressure Signature and other Tunnel Constraint Correction Methods for High Angle-of-Attack Tests", AGARD Report No.692, May 1980.

[4]Hackett, J. E., "Living with Solid-Walled Wind Tunnels", AIAA-82-0583, presented at the AIAA 12th Aerodynamic Testing Conference, March 22-24, 1982/Williamsburg, Virginia.

[5]Allmaras, S. R., "On Blockage Corrections for Two-Dimensional Wind Tunnel Tests using the Wall Pressure Signature Method", NASA-TM-86759, March 1986.

[6]Ashley, H. and Landahl, M., "Aerodynamics of Wings and Bodies", Addison-Wesley Publishing Company, Reading Massachusetts, p.129, Eq.(7-14).

[7]Schlichting, H. and Truckenbrodt, E., "Aerodynamics of the Airplane", translated by H. J. Ramm, McGraw-Hill Intl. Book Company, p.71, Eq.(2-97).

[8]Katz, J. and Plotkin, A., "Low-Speed Aerodynamics - From Wing Theory to Panel Methods", McGraw-Hill Intl. Book Company, 1991, p.60, Eq.(3.26).

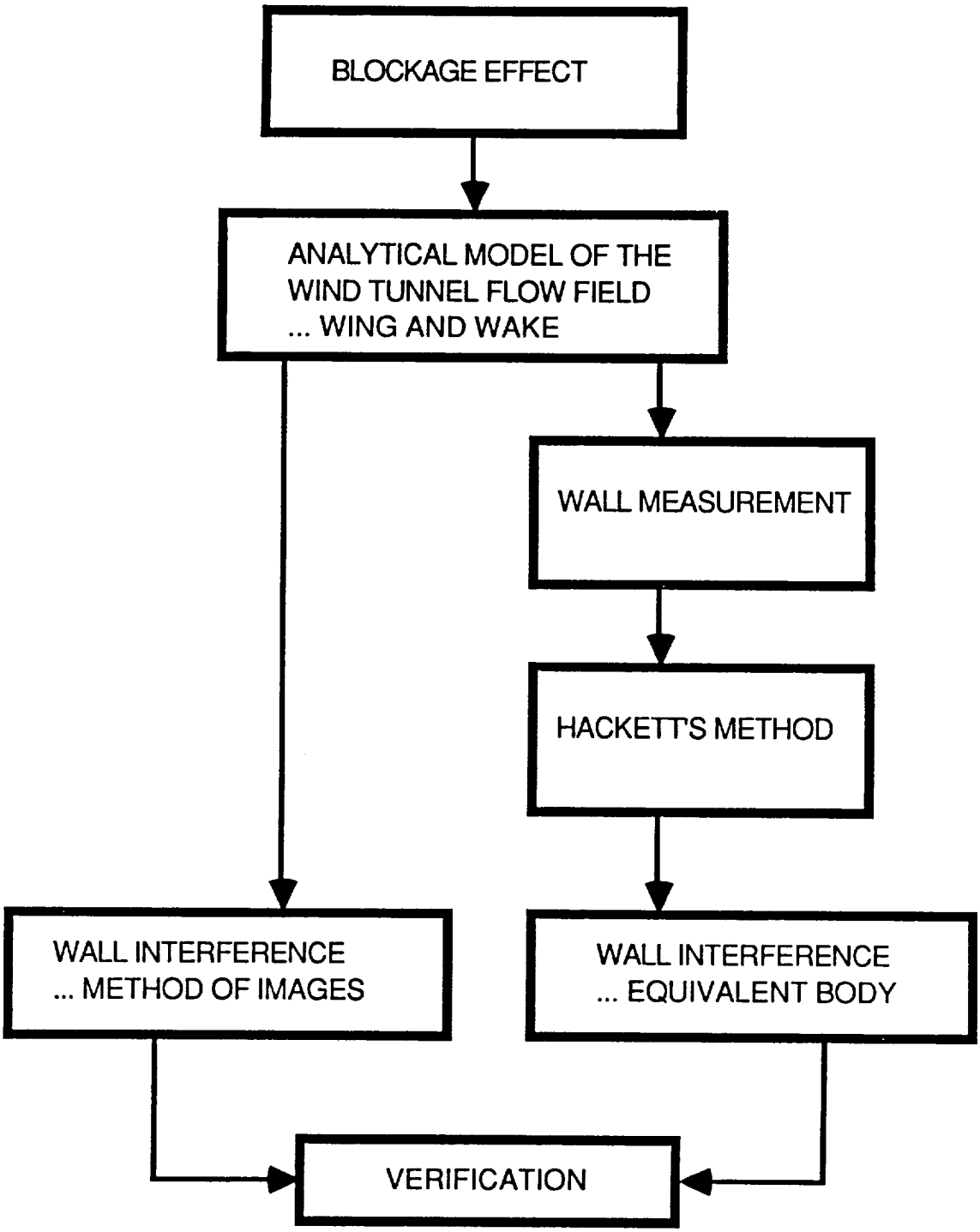

Fig. 1 Development and Verification of a 3-Dimensional Blockage Correction Technique

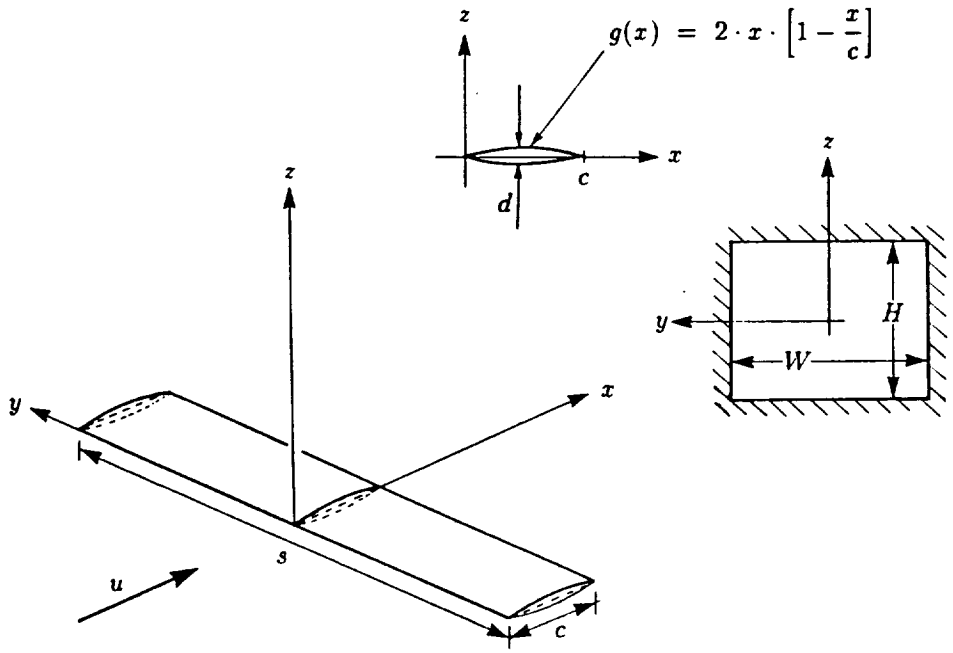

Fig. 2 Wing and Wind Tunnel Geometry

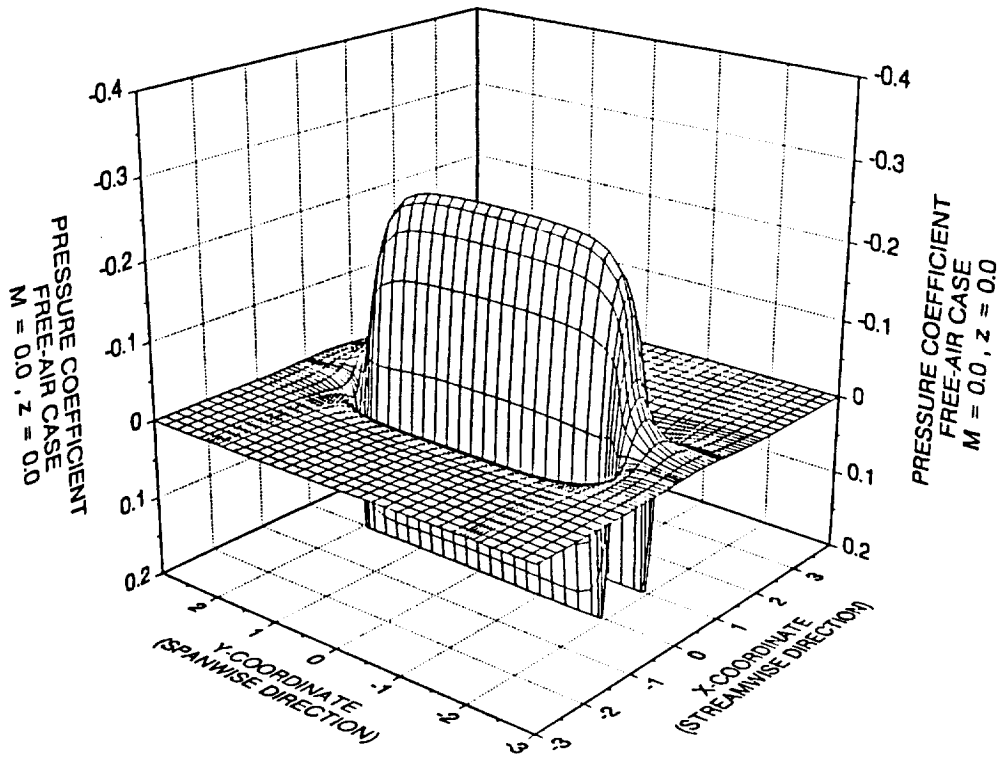

Fig. 3a Pressure Coefficient (Free-Air Case, $z = 0.0$)

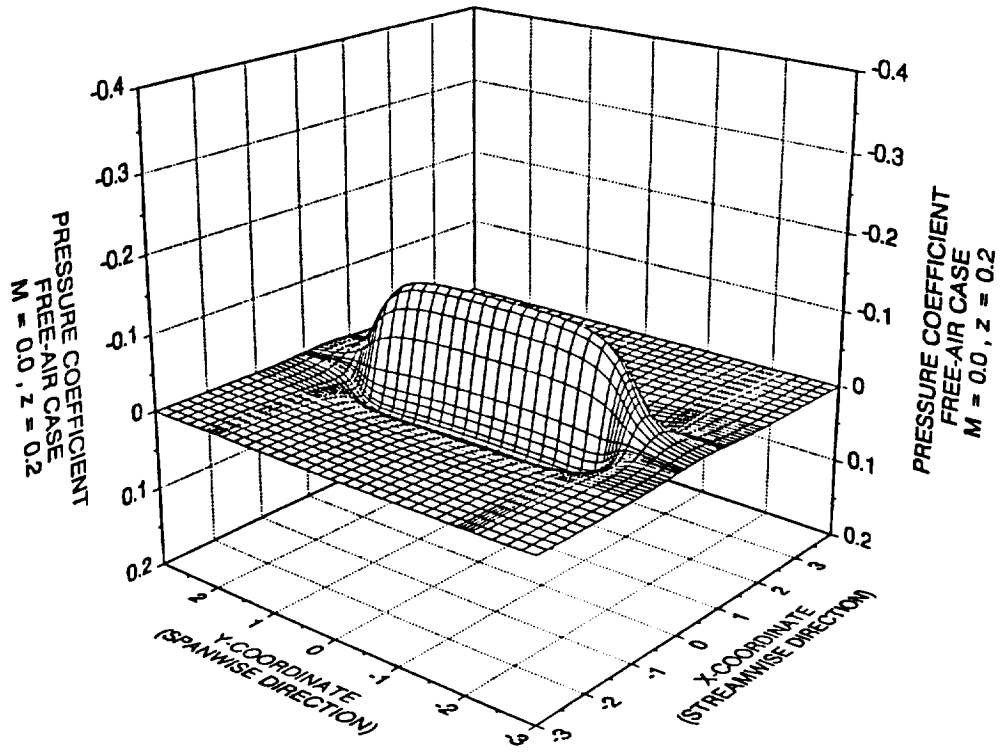

Fig. 3b Pressure Coefficient (Free-Air Case, $z = 0.2$)

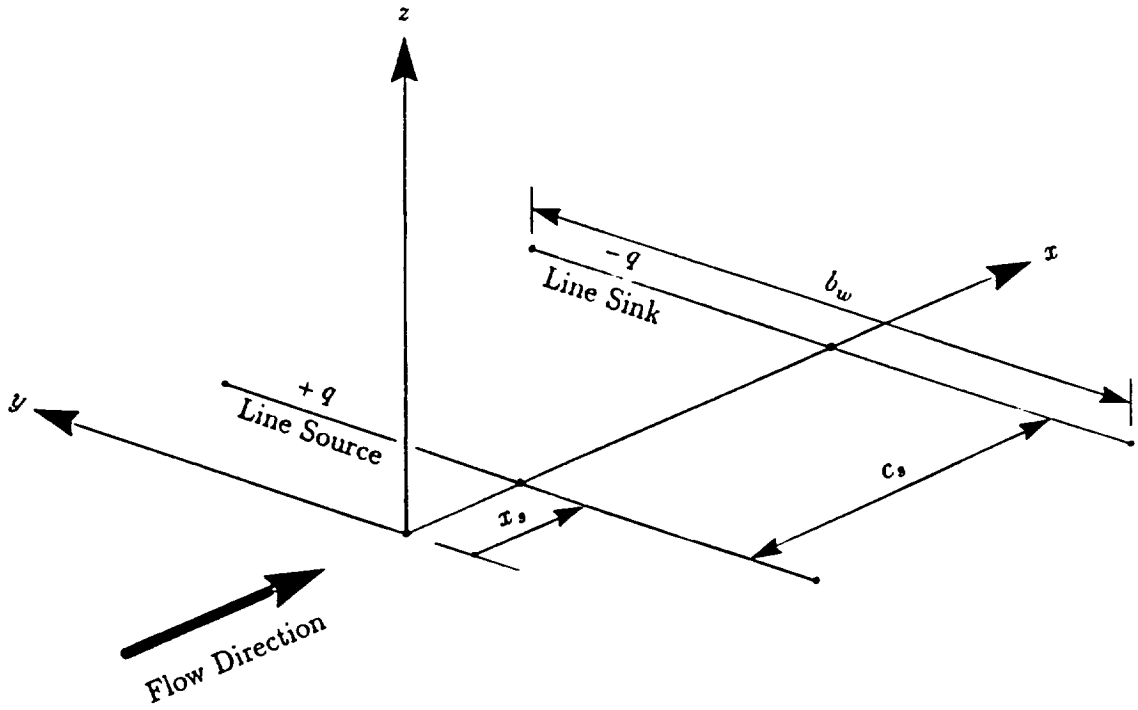

Fig. 4 Wake Model

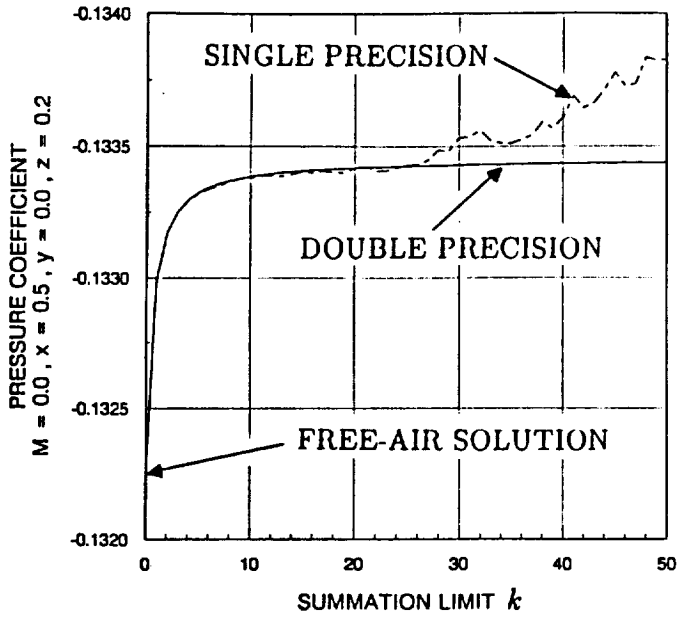

Fig. 5 Convergence of the Wind Tunnel Solution

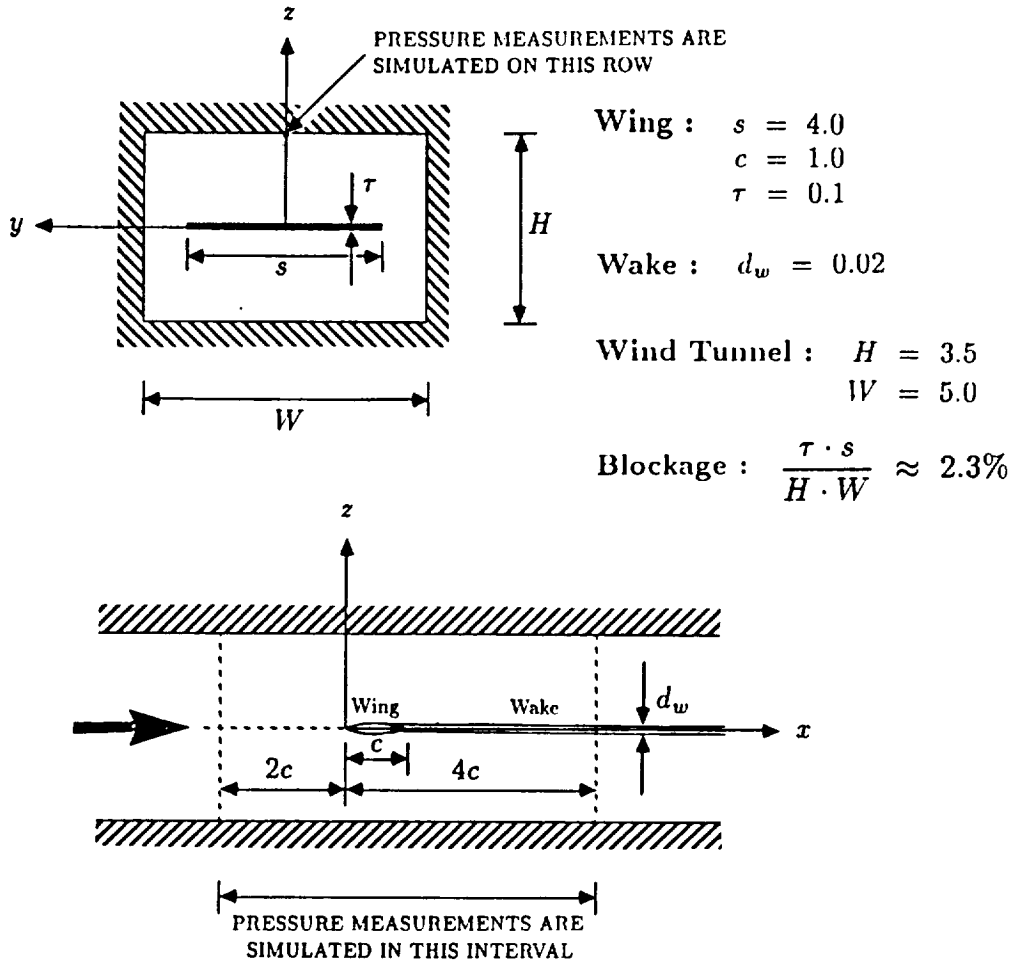

Fig. 6 Wing, Wake and Wind Tunnel Geometry

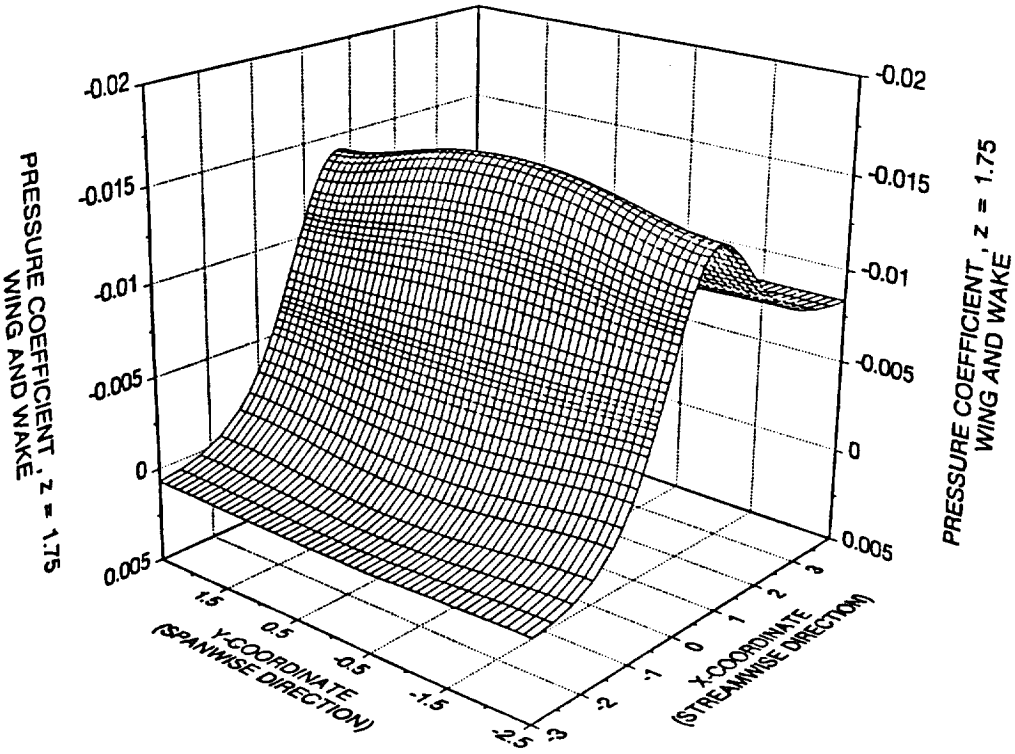

Fig. 7 Simulated Wall Pressure Measurements; $z = 1.75$

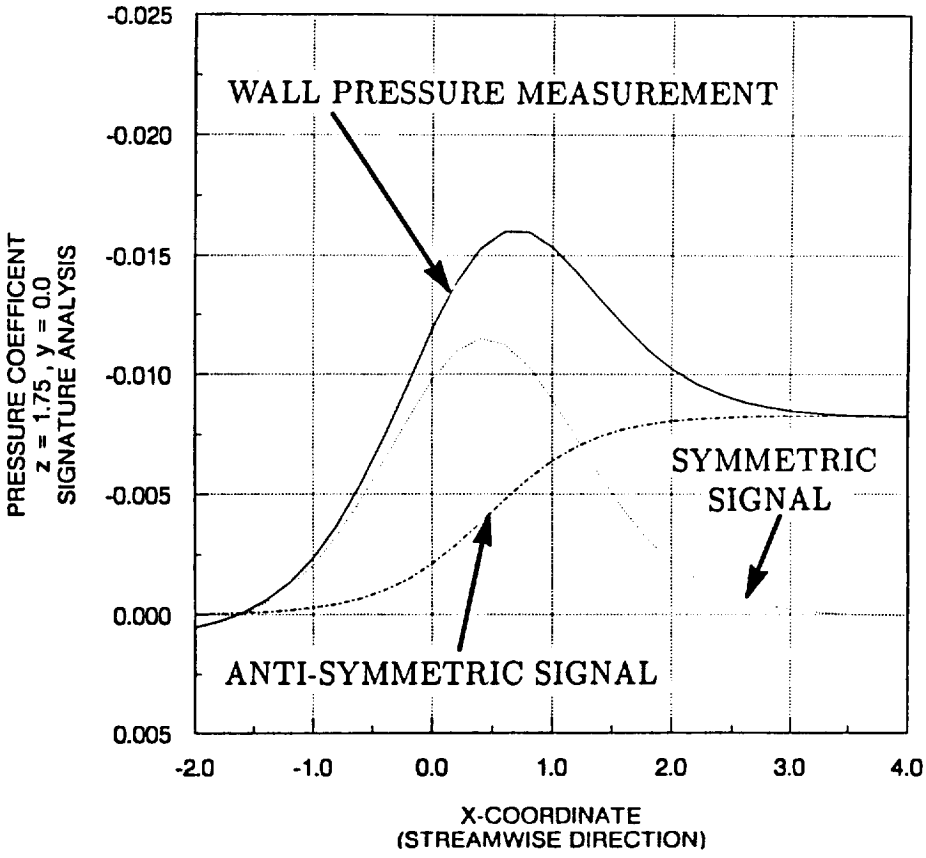

Fig. 8 Signature Analysis

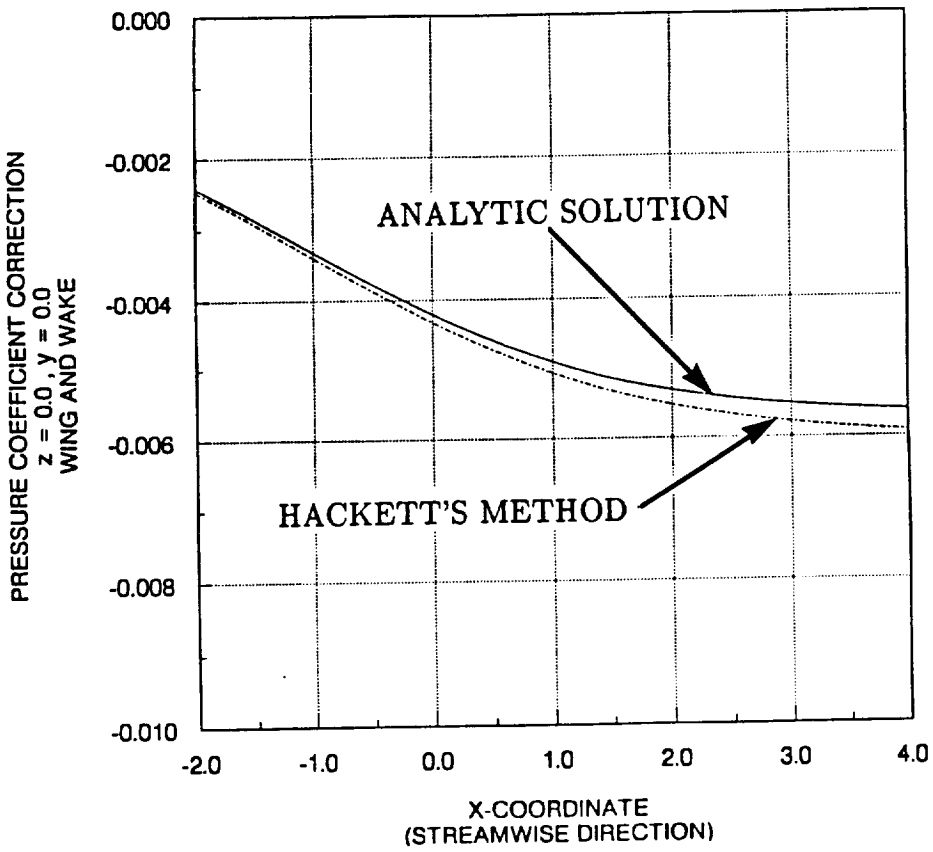

Fig. 9 Comparison of Pressure Coefficient Correction

APPENDIX A

ANALYTIC FLOW FIELD SOLUTION (WING)

Case No.	Condition	Solution
1	x arbitrary $\|y\| \neq s/2$ $z \neq 0$	Eq. (A.1)
2	x arbitrary $\|y\| = s/2$ $z \neq 0$	Eq. (A.2)
3	$x \neq 0$ and $x \neq c$ $\|y\| \neq s/2$ $z = 0$	Eq. (A.3)
4	$x \neq 0$ and $x \neq c$ $\|y\| = s/2$ $z = 0$	Eq. (A.4)
5	$x = 0$ or $x = c$ $\|y\| > s/2$ $z = 0$	Eq. (A.5)
6	$x = 0$ or $x = c$ $\|y\| \leq s/2$ $z = 0$	singular

$$u_1(x,y,z) = \frac{\tau}{\pi} \cdot [\, T_1 - T_2 - T_3 + T_4 \,] \qquad (A.1)$$

$$T_1 = \frac{1}{2} \cdot \frac{y+s/2}{|y+s/2|} \cdot \ln\left[\frac{S_1 - |y+s/2|}{S_1 + |y+s/2|} \cdot \frac{S_2 + |y+s/2|}{S_2 - |y+s/2|}\right]$$

$$T_2 = \frac{2}{c} \cdot (y+s/2) \cdot \left(x \cdot \frac{T_1}{y+s/2} - \ln\left[\frac{x+S_1}{(x-c)+S_2}\right] + \frac{|z|}{|y+s/2|} \cdot \left[\arctan\left(\frac{|y+s/2|}{|z|} \cdot \frac{x}{S_1}\right) - \arctan\left(\frac{|y+s/2|}{|z|} \cdot \frac{x-c}{S_2}\right)\right]\right)$$

$$T_3 = \frac{1}{2} \cdot \frac{y-s/2}{|y-s/2|} \cdot \ln\left[\frac{S_3 - |y-s/2|}{S_3 + |y-s/2|} \cdot \frac{S_4 + |y-s/2|}{S_4 - |y-s/2|}\right]$$

$$T_4 = \frac{2}{c} \cdot (y-s/2) \cdot \left(x \cdot \frac{T_3}{y-s/2} - \ln\left[\frac{x+S_3}{(x-c)+S_4}\right] + \frac{|z|}{|y-s/2|} \cdot \left[\arctan\left(\frac{|y-s/2|}{|z|} \cdot \frac{x}{S_3}\right) - \arctan\left(\frac{|y-s/2|}{|z|} \cdot \frac{x-c}{S_4}\right)\right]\right)$$

$$S_1 = \sqrt{x^2 + (y+s/2)^2 + z^2} \qquad S_2 = \sqrt{(x-c)^2 + (y+s/2)^2 + z^2}$$

$$S_3 = \sqrt{x^2 + (y-s/2)^2 + z^2} \qquad S_4 = \sqrt{(x-c)^2 + (y-s/2)^2 + z^2}$$

$$u_1(x,y,z) = \frac{\tau}{\pi} \cdot [\, T_1 + T_2 + T_3 \,] \qquad (A.2)$$

$$T_1 = \left[\frac{1}{2} - \frac{x}{c}\right] \cdot \ln\left[\frac{\sqrt{x^2+s^2+z^2} - s}{\sqrt{x^2+s^2+z^2} + s} \cdot \frac{\sqrt{(x-c)^2+s^2+z^2} + s}{\sqrt{(x-c)^2+s^2+z^2} - s}\right]$$

$$T_2 = \frac{2 \cdot s}{c} \cdot \ln\left[\frac{x + \sqrt{x^2+s^2+z^2}}{(x-c) + \sqrt{(x-c)^2+s^2+z^2}}\right]$$

$$T_3 = \frac{2 \cdot |z|}{c} \cdot \left[-\arctan\left(\frac{x \cdot s}{|z| \cdot \sqrt{x^2+s^2+z^2}}\right) + \arctan\left(\frac{(x-c) \cdot s}{|z| \cdot \sqrt{(x-c)^2+s^2+z^2}}\right)\right]$$

$$u_1(x,y,z) = \frac{\tau}{\pi} \cdot [\, T_1 + T_2 - T_3 - T_4 \,] \qquad (A.3)$$

$$T_1 = \frac{1}{2} \cdot \frac{y+s/2}{|y+s/2|} \cdot \left[1 - \frac{2x}{c}\right] \cdot \ln\left[\frac{S_1 - |y+s/2|}{S_1 + |y+s/2|} \cdot \frac{S_2 + |y+s/2|}{S_2 - |y+s/2|}\right]$$

$$T_2 = \frac{2}{c} \cdot (y+s/2) \cdot \ln\left[\frac{x + S_1}{(x-c) + S_2}\right]$$

$$T_3 = \frac{1}{2} \cdot \frac{y-s/2}{|y-s/2|} \cdot \left[1 - \frac{2x}{c}\right] \cdot \ln\left[\frac{S_3 - |y-s/2|}{S_3 + |y-s/2|} \cdot \frac{S_4 + |y-s/2|}{S_4 - |y-s/2|}\right]$$

$$T_4 = \frac{2}{c} \cdot (y-s/2) \cdot \ln\left[\frac{x + S_3}{(x-c) + S_4}\right]$$

$$S_1 = \sqrt{x^2 + (y+s/2)^2} \qquad S_2 = \sqrt{(x-c)^2 + (y+s/2)^2}$$

$$S_3 = \sqrt{x^2 + (y-s/2)^2} \qquad S_4 = \sqrt{(x-c)^2 + (y-s/2)^2}$$

$$u_1(x,y,z) \;=\; \frac{\tau}{\pi}\cdot[\;T_1 \;+\; T_2\;] \qquad (A.4)$$

$$T_1 \;=\; \frac{1}{2}\cdot\left[1-\frac{2x}{c}\right]\cdot\ln\left[\frac{\sqrt{x^2+s^2}-s}{\sqrt{x^2+s^2}+s}\cdot\frac{\sqrt{(x-c)^2+s^2}+s}{\sqrt{(x-c)^2+s^2}-s}\right]$$

$$T_2 \;=\; \frac{2\cdot s}{c}\cdot\ln\left[\frac{x+\sqrt{x^2+s^2}}{(x-c)+\sqrt{(x-c)^2+s^2}}\right]$$

$$u_1(x,y,z) \;=\; \frac{\tau}{\pi}\cdot[\;T_1 \;+\; T_2 \;+\; T_3 \;-\; T_4\;] \qquad (A.5)$$

$$T_1 \;=\; \frac{1}{2}\cdot\frac{y+s/2}{|y+s/2|}\cdot\ln\left[\frac{\sqrt{c^2+(y-s/2)^2}-|y-s/2|}{\sqrt{c^2+(y-s/2)^2}+|y-s/2|}\cdot\frac{\sqrt{c^2+(y+s/2)^2}+|y+s/2|}{\sqrt{c^2+(y+s/2)^2}-|y+s/2|}\right]$$

$$T_2 \;=\; \frac{y+s/2}{|y+s/2|}\cdot\ln\left[\frac{|y-s/2|}{|y+s/2|}\right]$$

$$T_3 \;=\; \frac{2}{c}\cdot(y+s/2)\cdot\ln\left[\frac{c+\sqrt{c^2+(y+s/2)^2}}{|y+s/2|}\right]$$

$$T_4 \;=\; \frac{2}{c}\cdot(y-s/2)\cdot\ln\left[\frac{c+\sqrt{c^2+(y-s/2)^2}}{|y-s/2|}\right]$$

APPENDIX B

CALCULATED LIMITS

$$\lim_{s\to\infty}\left[\frac{y+s/2}{|y+s/2|}\right] = 1 \qquad (B.1)$$

$$\lim_{s\to\infty}\left[\frac{y-s/2}{|y-s/2|}\right] = -1 \qquad (B.2)$$

$$\lim_{s\to\infty}\left[\frac{\sqrt{(x-c)^2+(y\pm s/2)^2}+|y\pm s/2|}{\sqrt{x^2+(y\pm s/2)^2}+|y\pm s/2|}\right] = 1 \qquad (B.3)$$

$$\lim_{s\to\infty}\left[\frac{\sqrt{x^2+(y\pm s/2)^2}-|y\pm s/2|}{\sqrt{(x-c)^2+(y\pm s/2)^2}-|y\pm s/2|}\right] = \frac{x^2}{(x-c)^2} \qquad (B.4)$$

$$\lim_{s\to\infty}\left[(y+s/2)\cdot\ln\left[\frac{x+\sqrt{x^2+(y+s/2)^2}}{(x-c)+\sqrt{(x-c)^2+(y+s/2)^2}}\right]\right] = c \qquad (B.5)$$

$$\lim_{s\to\infty}\left[(y-s/2)\cdot\ln\left[\frac{x+\sqrt{x^2+(y-s/2)^2}}{(x-c)+\sqrt{(x-c)^2+(y-s/2)^2}}\right]\right] = -c \qquad (B.6)$$

APPENDIX C

ANALYTIC FLOW FIELD SOLUTION (WAKE)

Case No.	Condition	Solution
1	$z \neq 0$ or $z = 0$ and $x \neq x_s$ and $x \neq x_s + c_s$	Eq. (C.1)
2	$z = 0$ and $x = x_s$ or $x = x_s + c_s$ and $\lvert y \rvert > b_w/2$	Eq. (C.2)
3	$z = 0$ and $x = x_s$ or $x = x_s + c_s$ and $\lvert y \rvert < b_w/2$	singular

$$u_2(x,y,z) = \frac{q}{4\pi} \cdot [\, A_1 - A_2 \,] \qquad (C.1)$$

$$A_1 = \frac{x - x_s}{(x - x_s)^2 + z^2} \cdot \left[\frac{y + b_w/2}{\sqrt{(x - x_s)^2 + (y + b_w/2)^2 + z^2}} - \frac{y - b_w/2}{\sqrt{(x - x_s)^2 + (y - b_w/2)^2 + z^2}} \right]$$

$$A_2 = \frac{x - x_s - c_s}{(x - x_s - c_s)^2 + z^2} \cdot \left[\frac{y + b_w/2}{\sqrt{(x - x_s - c_s)^2 + (y + b_w/2)^2 + z^2}} - \frac{y - b_w/2}{\sqrt{(x - x_s - c_s)^2 + (y - b_w/2)^2 + z^2}} \right]$$

$$u_2(x,y,z) = \frac{q}{4\pi} \cdot \frac{1}{c_s} \cdot \left[\frac{y + b_w/2}{\sqrt{{c_s}^2 + (y + b_w/2)^2}} - \frac{y - b_w/2}{\sqrt{{c_s}^2 + (y - b_w/2)^2}} \right] \qquad (C.2)$$